



Article

Spatiotemporal Heterogeneity in Runoff Dynamics and Its Drivers in a Water Conservation Area of the Upper Yellow River Basin over the Past 35 Years

Biao Zeng ¹, Fuguang Zhang ^{1,*}, Weifeng Zeng ², Ke Yan ¹ and Chengyu Cui ¹

¹ College of Earth and Environmental Sciences, Lanzhou University, Lanzhou 730000, China; zengb@lzu.edu.cn (B.Z.); yank20@lzu.edu.cn (K.Y.); cuichy20@lzu.edu.cn (C.C.)

² China Water Resources Beifang Investigation, Design and Research Company Limited, Tianjin 300222, China; zeng_wf@bidr.com.cn

* Correspondence: zhangfg15@lzu.edu.cn

Abstract: The upper Yellow River Basin (UYRB) is an important water source and conservation area. As well as a warming climate, the region has experienced long-term human interventions, such as grazing, farming and reservoir construction, since the mid-1980s. The runoff dynamics and its drivers in the UYRB remain poorly constrained, especially the differences between pastoral and agricultural areas, due to a lack of detailed measurements. Here, the contributions of climate change, land-use change and anthropogenic water consumption to runoff changes observed at hydrological stations were evaluated by combining the observations with scenarios simulated by a process-based hydrological model. Changes in the pastoral and agricultural areas of the UYRB were then compared at 10-year intervals during the period 1986–2020. The results indicated lower runoff in the UYRB over the past 35 years, when compared with that in the baseline period of 1965–1985, due to the negative influences of both climate change and anthropogenic water consumption. Meanwhile, land-use change had only a weak influence, due to stable land-use patterns. However, spatial differences in dominant drivers of runoff reductions were evident between the pastoral area and agricultural area. Specifically, runoff decreases were caused by the negative influences of climate change in the pastoral area and anthropogenic water consumption in the agricultural area. A shift in the dominant drivers after the period 2006–2015 was attributed to the positive influence of climate change and a weakening of agricultural water consumption and reservoir inflow during the same period. These changes initially caused a decrease in runoff, and later an increase. These findings contribute to a crucial evidence base for optimizing water resource management, ecological protection and high-quality development in the Yellow River Basin.

Keywords: runoff dynamics; dominant drivers; spatiotemporal heterogeneity; upper Yellow River Basin



Citation: Zeng, B.; Zhang, F.; Zeng, W.; Yan, K.; Cui, C. Spatiotemporal Heterogeneity in Runoff Dynamics and Its Drivers in a Water Conservation Area of the Upper Yellow River Basin over the Past 35 Years. *Remote Sens.* **2022**, *14*, 3628. <https://doi.org/10.3390/rs14153628>

Academic Editor: Giovanni Battista Chirico

Received: 17 June 2022

Accepted: 26 July 2022

Published: 29 July 2022

Publisher's Note: MDPI stays neutral with regard to jurisdictional claims in published maps and institutional affiliations.



Copyright: © 2022 by the authors. Licensee MDPI, Basel, Switzerland. This article is an open access article distributed under the terms and conditions of the Creative Commons Attribution (CC BY) license (<https://creativecommons.org/licenses/by/4.0/>).

1. Introduction

The Yellow River (Huang Ho) is central to Chinese culture, where it is considered the Mother River. The upper Yellow River Basin, as an important water source area and water conservation area [1–3], is a primary resource for socioeconomic development along the Yellow River [2,4]. The basin has experienced continuous agricultural and grazing activities, as well as a warming climate, over the past decades [5–7]. Agriculture in this region depends heavily on the upper Yellow River water resource [4,8], such that water consumption for livestock grazing has a direct impact on river runoff. Meanwhile, grazing also changes the underlying surface conditions (mainly the vegetation cover and soil structure), thereby influencing the local water cycle [2,9,10]. A series of ecological conservation and restoration programs (e.g., the Grain for Green Project and Grazing withdraw program) had additional impacts on the ground surface, with corresponding impacts on the water storage capacity

and runoff characteristics in this basin [4,11,12]. The construction of reservoirs has also caused intra- and inter-annual fluctuations in runoff [3,13].

Annual runoff of the upper Yellow River showed a reduction over the past several decades, while that of the river source regions of the Indus, Mekong, Salween, Ganges, Yarlung Zangbo, Amu Darya, Syr Darya and Tarim Rivers had obvious inter-annual variations but no significant trends [1,14,15]. Moreover, anthropogenic water consumption in these river source regions that originated from the Tibetan Plateau and its surroundings, known as the Asia water tower, was mainly concentrated in the upper Yellow River Basin [1,14]. Strong hydrological changes in the upper Yellow River Basin since the mid-1980s reflect the dual impacts of climate change and human activity [2,6,15,16]. Therefore, an improved understanding of runoff dynamics and drivers in the upper Yellow River Basin is urgently needed to reduce demand and optimize water resource management, in turn supporting ecological protection and high-quality development in the Yellow River Basin.

Previous studies revealed the general temporal characteristics of runoff changes across the entire upper Yellow River Basin, using hydrological station observations [2,3,16], and have qualitatively evaluated the contributions of climate change and human activity to these runoff changes [4,6,17]. However, the spatiotemporal differences in runoff changes between agricultural and pastoral areas within the upper Yellow River Basin remain poorly constrained, yet this knowledge is essential for decision-makers when regulating water resources [18]. The lack of quantitative data on the difference in runoff between pastoral and agricultural areas reflects a lack of relevant observations [2,12,19]. Nevertheless, some quantitative analysis has already been carried out. The elasticity coefficient method was established based on the Budyko hypothesis for the water balance and employed to measure the contributions of climate change and human activity to runoff changes [19–21]. The cumulative slope method was also widely used to quantify these two contributions by calculating the slopes of fitting lines before and after turning points in series of runoff, precipitation and evaporation [22]. This mathematical analysis has insufficient physical basis, due to a lack of knowledge of hydrological processes and their interactions [12,22,23], and its results remain uncertain. Additionally, detailed measurements of the individual contributions of climate change, land-use change and anthropogenic water consumption are rare in the upper Yellow River Basin, especially at different spatiotemporal scales. Previous measurements have focused more on the influences of climate change and land-use change [19,21,24]. Significantly, anthropogenic water consumption data are often difficult to collect directly [25], yet they provide critical information for policymakers regulating water resources in the Yellow River Basin [2,18]. Additionally, the land-use change in the previous studies generally included variations in native vegetation cover associated with climate change, which exaggerated the contribution of land-use change caused solely by human activities [19–21].

Process-based eco-hydrological simulations of specific scenarios provide an effective means of measuring the individual contributions of climate change, land-use change and anthropogenic water consumption to runoff changes. Models can be employed to simulate runoff dynamics driven jointly by both climate change and land-use change at the watershed scale, using observed climate and land-use time series [2,25]. Runoff dynamics driven solely by climate change can also be simulated, by keeping land-use constant at its initial state throughout the simulation [19,26]. The contributions of climate change, land-use change and anthropogenic water consumption to runoff changes are then quantified by comparing the simulated runoff series with observed runoff series at hydrological stations. The Soil and Water Assessment Tool (SWAT) has been widely applied to implement these simulations at the watershed and sub-watershed scales and had a good performance in our study in the Asia water tower region [22,27–29].

This study aims to evaluate spatiotemporal differences in runoff dynamics and its drivers within a water conservation area of the upper Yellow River Basin over the past 35 years. The runoff series were generated by the SWAT model, based on two scenarios

that were constructed by observed climatic series and with or without land-use status at 10-year intervals during the period 1986–2020. The changes in simulated and observed runoff series were quantified by comparing with that in the baseline period of 1965–1985. The dominant drivers were then identified by comparisons of these runoff changes as noted above. The differences between agricultural areas and pastoral areas were further analyzed. These results are expected to support optimization of water resources regulation in the Yellow River Basin.

2. Materials and Methods

2.1. Study Area

The upper Yellow River Basin above the Lanzhou hydrological station (UYRB) is located at latitude $32^{\circ}09'14''$ – $38^{\circ}20'52''$ N and longitude $95^{\circ}52'27''$ – $103^{\circ}50'08''$ E, with a total catchment area of approximately 223,000 km², accounting for 29.7% of the whole Yellow River Basin (Figure 1). The UYRB is the main source of runoff to the Yellow River, yielding about 60% of the mean annual runoff [2,30]. This basin also has an important water conservation function [12]. The UYRB features a plateau mountain climate, and over the past 70 years has experienced increasing precipitation (approximately 4.85 mm per decade) and warming (approximately 0.12 °C per decade) [2,3]. Grassland, forest land and cropland are the main land-use types, accounting for 79.19%, 12.13% and 6.46% of this basin, respectively (Figure 2). Animal husbandry and agriculture are the main pillar industries of local socioeconomic developments [31]. Grazing and farming activities are respectively concentrated in the sub-basins above and below the Tangnaihai hydrological station in the UYRB (Figure 2). Agricultural irrigation accounts for the majority of anthropogenic water consumption, but domestic water and industrial water have followed an increasing trend [6]. Several reservoirs have been successively built in the sub-basin below the Tangnaihai hydrological station since 1986 [3].

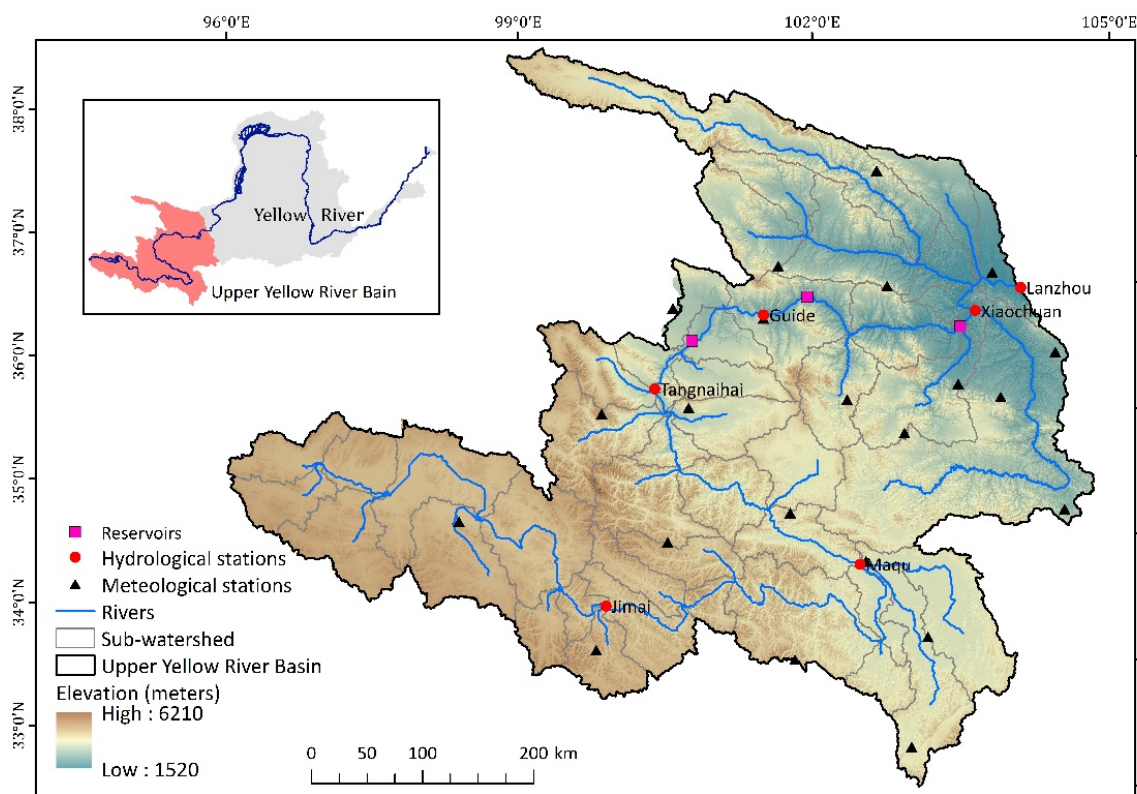


Figure 1. The upper Yellow River Basin.

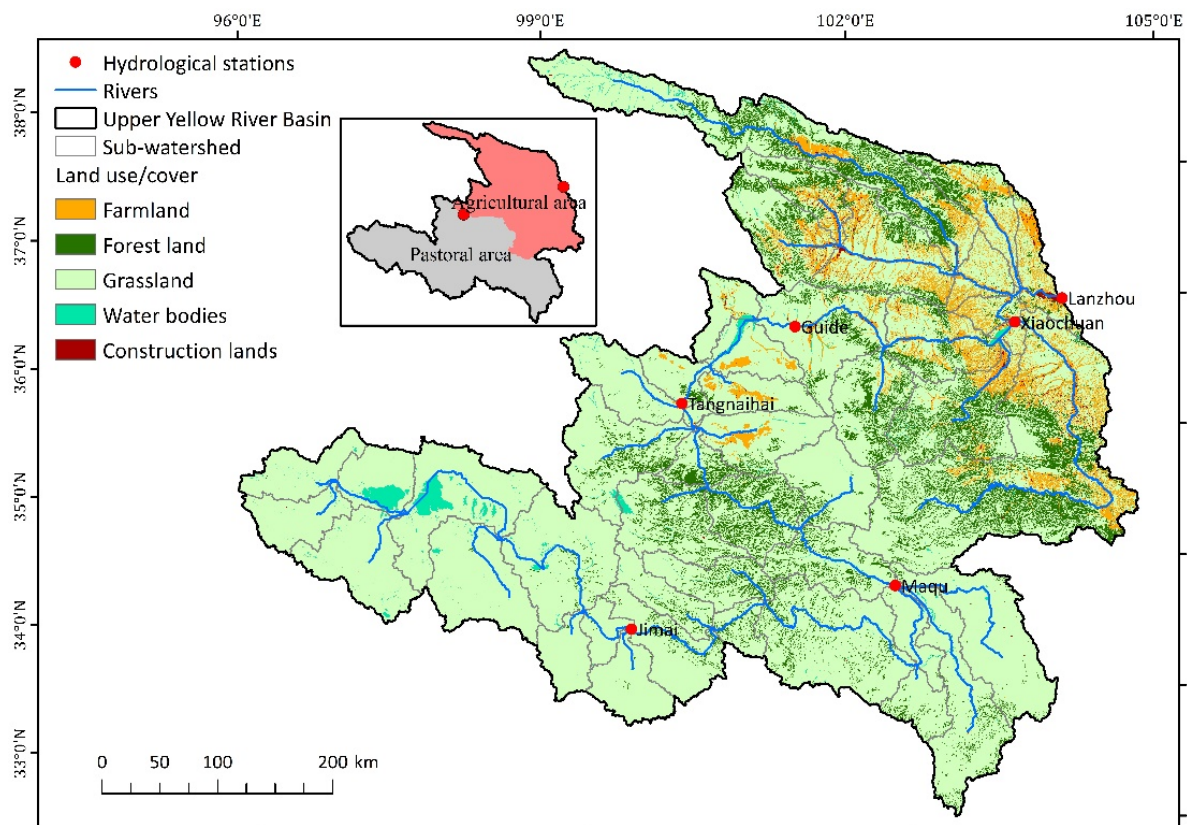


Figure 2. Major types of land-use map from 1990s to 2020s.

2.2. Data

2.2.1. Observed Runoff Series

Monthly streamflow series from six hydrological stations (Figure 1) within the UYRB during 1965–2020 were obtained from the Yellow River Conservancy Commission of China (the agency responsible for quality control and release of the hydrological data). These data series recorded observed runoff in the study area, which reflects the joint influences of climate change, land-use change and anthropogenic water consumption. The data were converted to a series of total annual runoff.

The monthly runoff series from 1965 to 1975 was used to calibrate parameters of the SWAT model, while the series from 1976 to 1985 was used for validation of runoff simulations.

The monthly runoff series for the Lanzhou hydrological station from 1986 to 2020 reflects overall runoff dynamics in the UYRB, while that from the Tangnaihai hydrological station was adopted to represent the pastoral area of the UYRB (Figure 2). The differences between these two runoff series were utilized to estimate changes in the runoff dynamics in the agricultural area of the UYRB.

2.2.2. Driving Datasets for Simulating Runoff Dynamics

Daily climatic series, land-use data, a soil survey geographical database and elevation data were required by the SWAT model to simulate runoff dynamics. Daily climatic variables (Table 1) included temperature, precipitation, solar radiation, relative humidity and wind speed at 22 meteorological stations (Figure 1) within the UYRB from 1964 to 2020, obtained from the China meteorological service center (<http://data.cma.cn/en> (accessed on 1 June 2022)).

Table 1. Climatic datasets for runoff simulations.

Climatic Datasets	Time Resolution	Unit	Timespan
Mean temperature	day	$^{\circ}\text{C}\cdot\text{day}^{-1}$	1964–2020
Total precipitation	day	$\text{mm}\cdot\text{day}^{-1}$	
Mean solar radiation	day	$\text{W}\cdot\text{m}^{-2}\cdot\text{day}^{-1}$	
Mean relative humidity	day	%	
Mean wind speed	day	$\text{m}\cdot\text{s}^{-1}$	

Land-use data in the UYRB, with a spatial resolution of 30 m for the years 1990, 2000, 2010 and 2020, were provided by the National Tibetan Plateau Data Center (<http://www.resdc.cn/> (accessed on 1 June 2022)). These data were produced by artificial visual interpretation using Landsat TM/ETM images over the same period. The land-use data are of high quality and have been widely applied in eco-hydrological research.

The soil survey geographical database provides physical and chemical characteristics of soils (e.g., percentages of clay, sand and silt and saturated hydraulic conductivity). We used the Harmonized World Soil Database version 1.2 from the International Institute for Applied Systems Analysis and Food and Agriculture Organization of the United Nations. The HWSD covers over 16,000 different soil mapping units and has high accuracy [32]. Delineation processes follow Winchell et al. (2010) [33].

The ASTER GDEM version 2 with a spatial resolution of approximately 30 m was obtained from NASA's Land Processes Distributed Active Archive Center. The data have high accuracy, even in mountainous areas, and have also been widely used in eco-hydrological models [34]. The elevation data extracted from this dataset were used as the model input.

2.2.3. Anthropogenic Water Consumption Data

Anthropogenic water consumption data were retrieved from statistics published by the Ministry of Water Resources. Water consumption data for agricultural irrigation, forestry, industry, domestic use and animal husbandry from 2004 to 2020 were included in the following analysis. Annual inflows of reservoirs that were built in the agricultural area of the UYRB from 2009 to 2020 were obtained from the Yellow River Conservancy Commission of China.

2.3. Method

2.3.1. Scenario Simulations for Quantifying Contributions of Individual Drivers to Runoff Dynamics

Monthly runoff dynamics in scenario simulations were simulated by the SWAT (semi-distributed watershed) model [27,35]. The SWAT model was driven by the climate, land-use and soil characteristics datasets. The mass balance, transport and hydrologic cycling were simulated for individual hydrological response units identified by their unique combinations of land-use, soil type and terrain characteristics. The surface runoff and infiltration were calculated by the soil conservation service curve number method [28,33]. The simulated runoff was routed to the watershed outlet through channel processes. Further details are found in Neitsch et al. [36].

(1) Model parameterization and validation

The monthly runoff series from 1964 to 1985 were simulated by this model using observed climate and land-use data as described above. The year 1964 was used for model initialization and spin-up. The land-use data were assigned their values for the year 1990, as there was little land development in the study area before the 1990s [2,16].

The simulation from 1965 to 1975 was employed to calibrate the model parameters at the six hydrological stations of the study area (see Figure 1) using the SWAT-CUP tool [37]. Firstly, sensitive parameters (Table 2) were determined by the degree and significance of sensitivity (i.e., *t*-stat and *p* value) from global sensitivity analysis of the SWAT-CUP [38]. Here, the significance was set to 0.1. Next, the 50–100 iterative simulations with the param-

eters were performed and compared with the observed runoff series in the corresponding period. The chosen values of these parameters were adjusted within a reasonable range as Table 1 to obtain the optimal parameters with minimum simulation error. Then, the model was run again with the calibrated parameter set to simulate runoff dynamics from 1976 to 1985. The simulated and observed series of monthly runoff were then compared to verify the reliability of the model. Note that the observed runoff series before 1985 was considered to reflect the sole influence of climate change, due to the weak human impacts during that period [15,16]. The Nash–Sutcliffe efficiency coefficient (NSE), coefficient of determination (R^2) and percent bias (PBIAS) were used as metrics in calibration and validation. Simulations are generally considered to be reliable when $0.75 \leq NSE \leq 1.0$, $R^2 \geq 0.75$ and $PBIAS \leq \pm 10\%$ [39].

Table 2. Parameters used for calibration in the SWAT model.

Parameters	Description	Value Range
r_CN2	Initial SCS runoff curve number for moisture condition II	[−0.2, 0.2]
v_ALPHA_BF	Baseflow alpha factor	[0, 1]
v_GW_DELAY	Groundwater delay time	[0, 500]
v_GW_REVAP	Groundwater “revap” coefficient	[0.02, 0.2]
v_GWQMN	Groundwater baseflow threshold (mm)	[0, 2000]
v_REVAPMN	Groundwater “revap” threshold (mm)	[0, 500]
v_CH_N2	Manning’s “n” value for the main channel	[0, 0.3]
v_OV_N	Manning’s “n” value for overland flow	[−0.01, 30]
v_CH_K2	Effective hydraulic conductivity in main channel alluvium	[0, 150]
v_ESCO	Soil evaporation compensation factor	[0.01, 1]
v_EPCO	Plant uptake compensation factor	[0.01, 1]
v_SMFMX	Maximum melt rate for snow during year	[0, 10]
v_SFTMP	Snowfall temperature	[−5, 5]

Notes: The prefix “r” means multiplied by a given value. The prefix “v” means replacement of the initial parameter with a given value.

(2) Scenario simulations

Scenarios 1 and 2 (Table 3) used observed climatic series during the corresponding time-span but were run with and without land-use change, respectively. The monthly runoff series in these scenarios were simulated by the calibrated SWAT model with the configuration shown in Table 3. Scenario 1 was driven solely by climate change, while Scenario 2 was driven jointly by climate change and land-use change. The simulated period 1986–2020 was subdivided into intervals of 10 years to reflect land-use change. The simulated results from these two scenarios were then compared to evaluate the contribution of land-use change to runoff changes.

Table 3. Scenario configurations.

Simulated Periods	Scenario 1	Scenario 2
1986–1995	observed climatic	1990 land use
1996–2005	series	observed climatic
2006–2015	and	series and
2016–2020	1990 land use	2020 land use

2.3.2. Quantifying the Contributions of Climate Change, Land-Use Change and Anthropogenic Water Consumption to Runoff Changes

The observed runoff series (R_A) before 1985 was considered to solely reflect the response to climate change, due to the weak human interventions during that period. The R_A during 1965–1985 (i.e., baseline period) was thus adopted as the benchmark from which to assess human impacts on runoff changes since 1986.

The observed runoff changes (ΔR_A) were quantified as the differences in annual mean R_A between the simulated periods (Table 3) and the baseline period. Therefore, ΔR_A reflects

the combined responses to climate change (ΔR_C), land-use change (ΔR_L) and anthropogenic water consumption (ΔR_U). Specifically,

$$\Delta R_A = \Delta R_C + \Delta R_L + \Delta R_U \quad (1)$$

ΔR_C was calculated as the differences in annual mean value between the simulated runoff series from Scenario 1 (see Table 3) and the R_A during the baseline period. ΔR_L was calculated as the difference in the simulated annual runoff between Scenario 1 and Scenario 2. ΔR_U was finally calculated as the residual after accounting for ΔR_A , ΔR_C and ΔR_L .

Fractional contributions of climate change, land-use change and anthropogenic water consumption were then quantified as FC_C , FC_L and FC_U .

$$FC_C = |\Delta R_C| / (|\Delta R_C| + |\Delta R_L| + |\Delta R_U|) \quad (2)$$

$$FC_L = |\Delta R_L| / (|\Delta R_C| + |\Delta R_L| + |\Delta R_U|) \quad (3)$$

$$FC_U = |\Delta R_U| / (|\Delta R_C| + |\Delta R_L| + |\Delta R_U|) \quad (4)$$

The dominant drivers of runoff changes were further explored by comparing the magnitudes of these individual contributions. To identify significant differences between contributions, we used a threshold minimum difference of 0.2 between the absolute values of the fractional contributions. The directions of the dominant drivers were also determined by the signs of ΔR_C , ΔR_L and ΔR_U , respectively. A positive sign indicated that the factor had a positive influence on runoff changes, and vice versa. The differences between the dominant drivers of change in the agricultural and pastoral areas were then analyzed in the UYRB.

3. Results

3.1. Reliability of Runoff Simulations

The monthly runoff series simulated by the SWAT model showed a good fit ($R^2 > 0.79$) with the observed runoff during both the calibration and validation period (Table 4). Overall, the calibrated SWAT model achieved high accuracy ($NSE > 0.77$ and $|PBIAS| < 10\%$) when simulating runoff dynamics in the UYRB and provided a reliable basis for the following drivers contribution analysis.

Table 4. Validation of annual runoff series simulated by the SWAT model in the upper Yellow River Basin.

Hydrological Stations	Calibration Period			Validation Period		
	NSE	R ²	PBIAS (%)	NSE	R ²	PBIAS (%)
Jimai	0.84	0.85	2.10	0.77	0.79	−3.25
Maqu	0.89	0.89	0.91	0.84	0.86	−6.52
Tangnaihai	0.89	0.90	−0.64	0.85	0.86	−8.81
Guide	0.90	0.91	−2.04	0.86	0.87	−9.03
Xiaochuan	0.90	0.90	−2.12	0.85	0.85	−0.84
Lanzhou	0.90	0.90	−3.7	0.87	0.87	−4.69

Notes: NSE, R² and PBIAS are the Nash–Sutcliffe efficiency coefficient, coefficient of determination and percent bias, respectively.

As shown in Figure 3, the monthly series of simulated runoff at the six hydrological stations during the calibration and validation periods were highly consistent with the respective observations. The hydrological processes simulation showed the characteristics of the monthly runoff, and in particular the high flows from June to October and low flows from November to April (Figure 3a–f). The simulated fluctuations of the monthly runoff at these hydrological stations were similar, but the flow variation was different, which yielded a good match with observations.

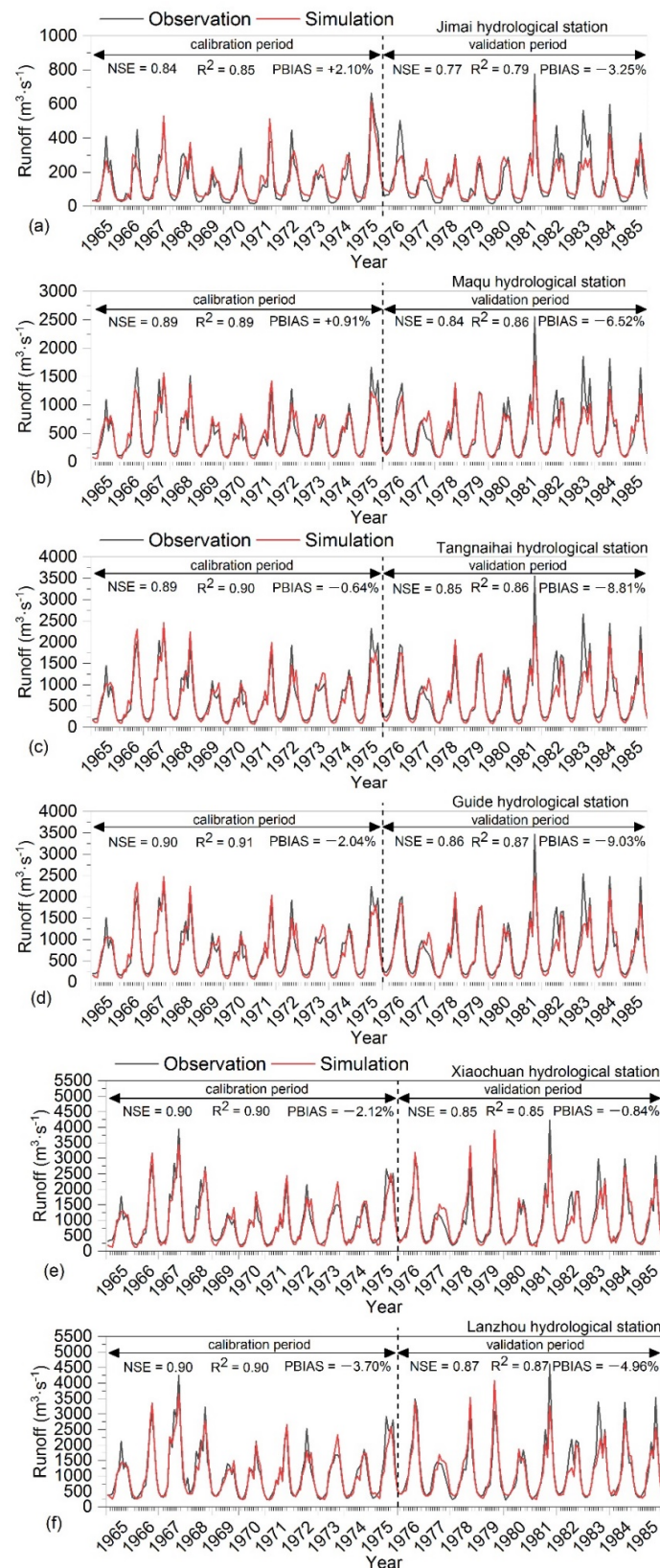


Figure 3. Observed and simulated runoff series during the calibration period (1965–1975) and validation period (1976–1985) at the hydrological stations in the upper Yellow River Basin. Comparisons of these two runoff series in (a) the Jimai, (b) Maqu, (c) Tangnaihai, (d) Guide, (e) Xiaochuan and (f) Lanzhou hydrological stations, respectively.

3.2. Runoff Characteristics and Their Spatiotemporal Variability

As shown in Figure 4, spatiotemporal differences in runoff changes from 1986 to 2020 were evident in the UYRB. The observed runoff from the entire UYRB during the period 1986–2020 showed a reduction of $64.87 \times 10^8 \text{ m}^3 \cdot \text{a}^{-1}$ compared with that in the baseline period of 1965–1985, mainly due to climate change and anthropogenic water consumption (Figure 4a). However, the reduction of observed runoff in pastoral areas was less than that in the agricultural area (Figure 4b,c). Evidently, the observed runoff changes in the pastoral and agricultural areas were mainly caused by climate change and anthropogenic water consumption, respectively (Figure 4b,c). The temporal characteristics of the observed runoff changes over the past 35 years appeared similar in the entire UYRB, and in the pastoral area and agricultural area: there was firstly a reduction and then an increase, before and after the period of 2006–2015 (Figure 4). The abrupt changes in observed runoff were attributed to positive contributions of climate change and a reduction of anthropogenic water consumption.

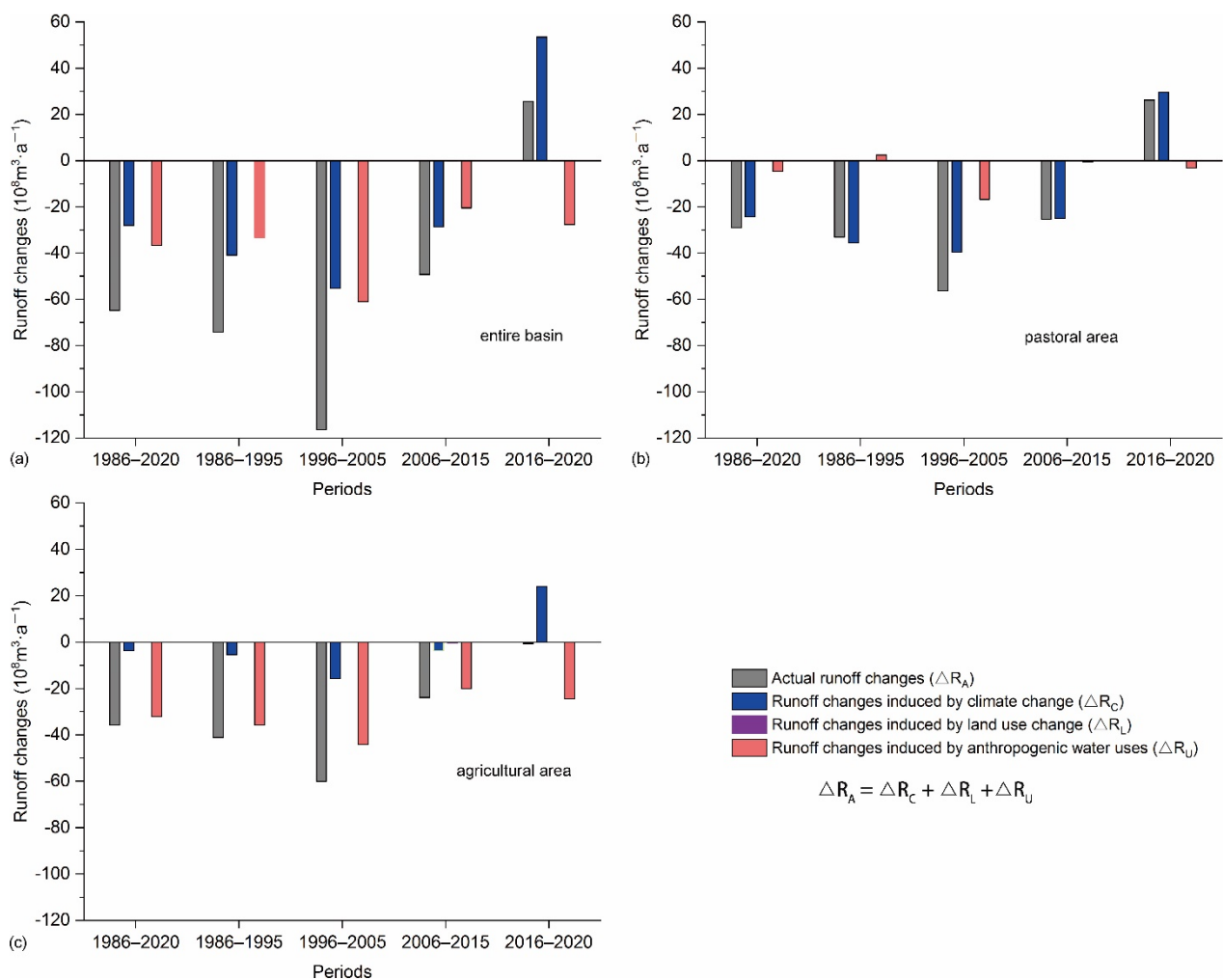


Figure 4. Runoff changes in the Upper Yellow River Basin during 1986–2020 compared with those in the baseline period (1965–1985). The runoff changes are attributed to climate change (ΔR_C), land-use change (ΔR_L) and anthropogenic water consumption (ΔR_U) in different periods in (a) the entire UYRB, (b) pastoral area and (c) agricultural area, respectively.

The runoff changes due to climate change (i.e., ΔR_C) in the entire UYRB during the period 1986–2020 were $-28.05 \times 10^8 \text{ m}^3 \cdot \text{a}^{-1}$ (Figure 4a), which indicated that climate change has caused decreasing runoff over the past 35 years. The decrease was mainly due to changes concentrated in the pastoral area (Figure 4b,c), which indicated that climate

change had greater contributions to runoff reductions here than in the agricultural area. Evidently, the runoff changes due to climate change led to a similar temporal pattern in observed runoff during the corresponding period in the UYRB (Figure 4). These runoff changes were generally consistent with precipitation changes in the corresponding periods, but were additionally altered by temperature changes (Figures 4a and 5a,b).

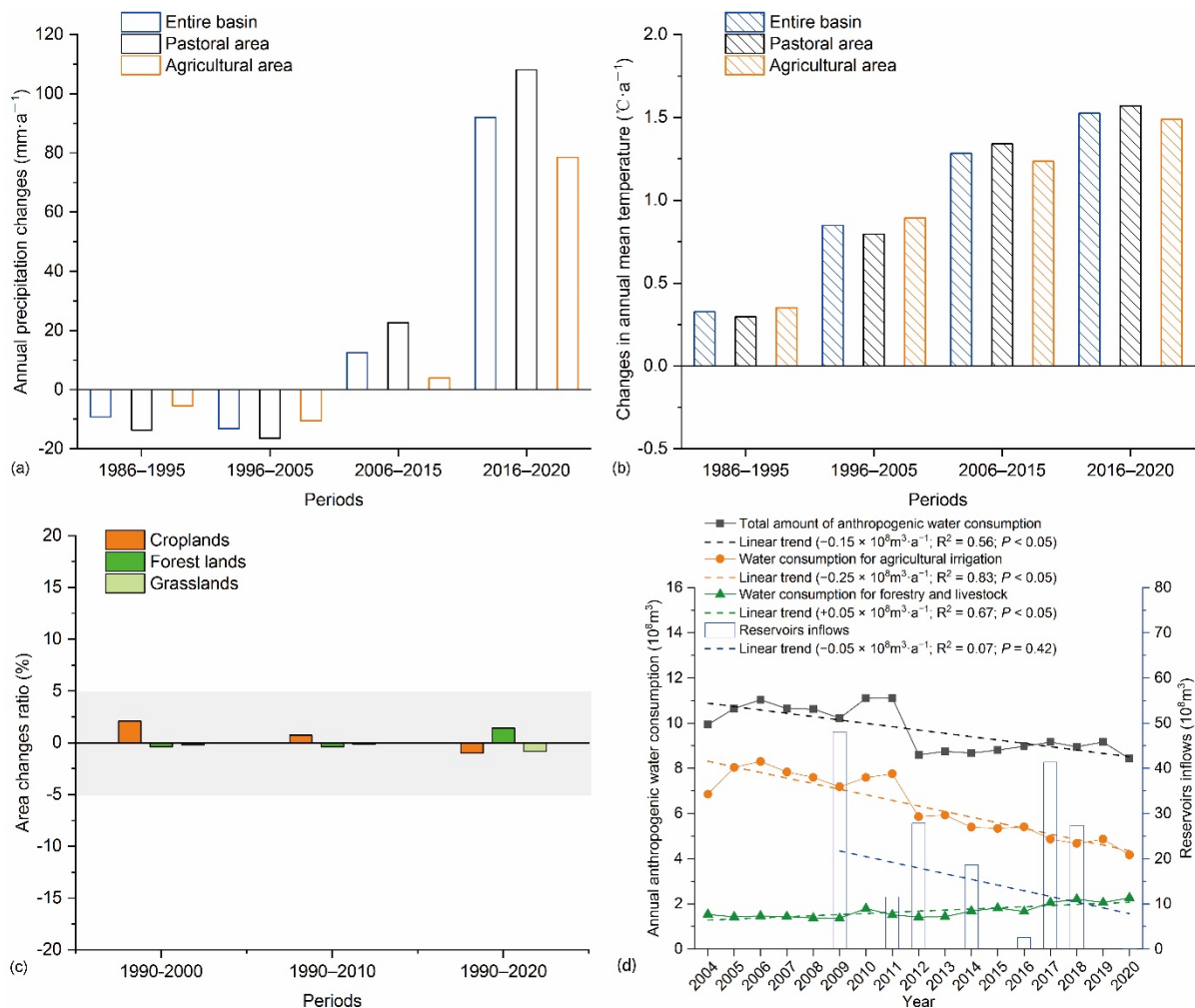


Figure 5. Changes in climate, land-use and anthropogenic water consumption during 1986–2020. Changes in (a) annual precipitation and (b) annual mean temperature in different periods compared with that in the baseline period (1965–1985). (c) Land-use change from 1990 to 2020. (d) Annual anthropogenic water consumption from 2004 to 2020, and annual inflows of reservoirs built in the agricultural area from 2009 to 2020.

The runoff changes induced by land-use change (i.e., ΔR_L) were unobvious in the UYRB over the past 35 years (Figure 4), which we attribute to a stable land-use pattern from 1990 to 2020 (Figure 5c). However, the runoff reduction due to anthropogenic water consumption was evident in the entire UYRB from 1986 to 2020 and showed an increase and then decrease before and after the period 1996–2005 (Figure 4). Total anthropogenic water consumption included water storage in reservoirs and showed a decrease since 2004 (Figure 5d). The runoff reduction due to anthropogenic water consumption in the period of 2006–2020 was equivalent to the sum of total water consumption and water storage in hydraulic projects in the agricultural area during the same period (Figures 4a and 5d). Moreover, agricultural irrigation accounts for the majority of anthropogenic water consumption (Figure 5d). Clearly, the runoff reductions due to anthropogenic water consumption were primarily concentrated in the agricultural area that depends on irrigation

(Figure 4b,c). These results indicated that reservoir regulation and agricultural irrigation are the main factors influencing anthropogenic water consumption and played strong roles in the runoff reduction in the agricultural area. Obviously, anthropogenic water consumption due to forestry and livestock accounts for about 17% of the total water consumption over the past 35 years (Figure 5d), which indicated that anthropogenic water consumption was relatively low in the pastoral area.

3.3. Spatiotemporal Heterogeneity of the Individual Contributions to Runoff Changes

Figure 6 illustrates the relative contributions of climate change, land-use change and anthropogenic water consumption to observed runoff changes in the UYRB from 1986 to 2020. The contributions of climate change and anthropogenic water consumption to observed runoff changes in the entire UYRB were similar over the past 35 years, but the contribution of land-use change was unobvious (Figure 6a). Climate change and anthropogenic water consumption are negative drivers, and exerted similar influences on the observed runoff reductions in the entire UYRB during the whole study period (Figures 4a and 6a,d). However, the dominant driver of observed runoff changes appeared to undergo a turning point during the period of 2006–2015: specifically, the observed runoff increased during the period 2016–2020, when compared with that of the baseline period of 1965–1985, due to the positive effects of climate change and weakened contributions of anthropogenic water consumption (Figure 6a,d).

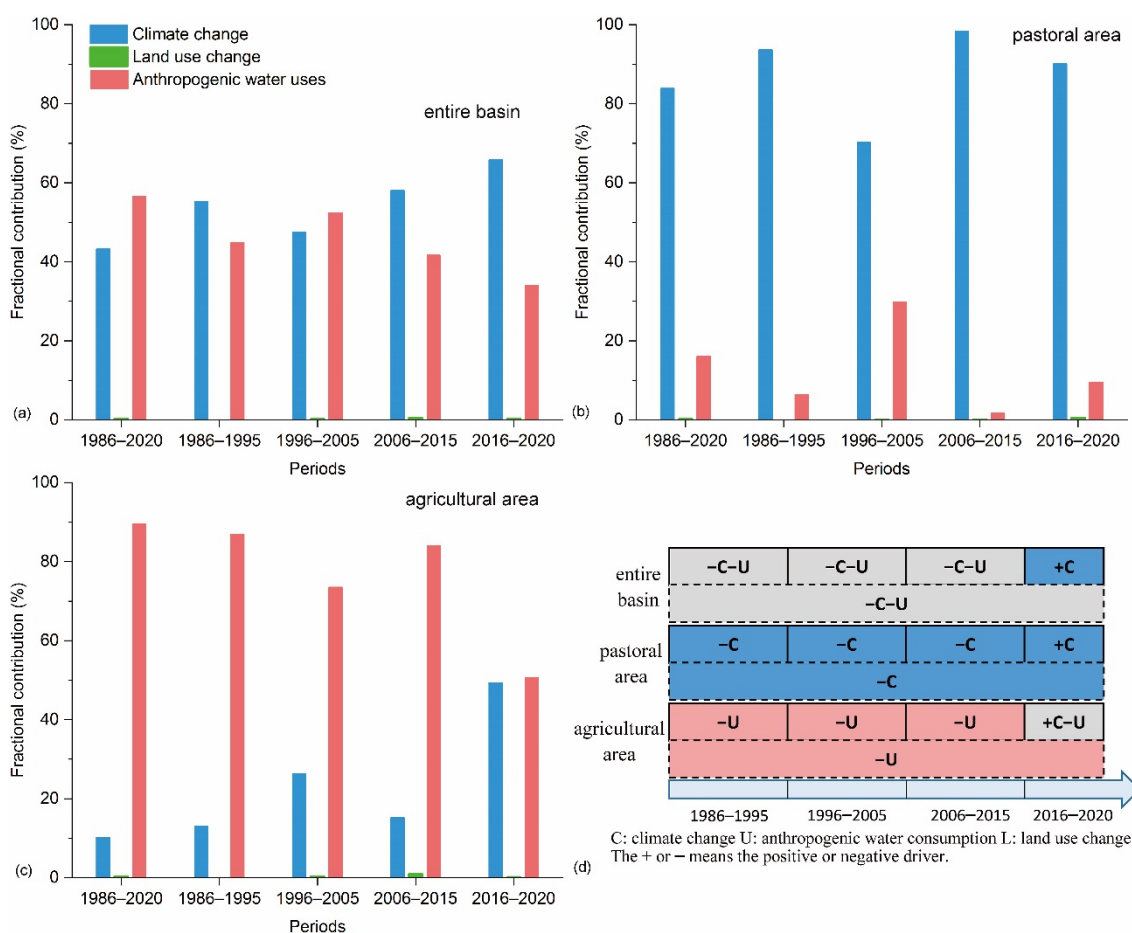


Figure 6. Relative contributions of climate change, land-use change and anthropogenic water uses to runoff changes in the upper Yellow River Basin from 1986 to 2020. The contributions are for (a) the entire UYRB, (b) pastoral area and (c) agricultural area, respectively. (d) Spatiotemporal variations of dominant drivers in this basin over the past 35 years.

In the pastoral area, the negative influence of climate change dominated runoff decreases during 1986–2020 (Figures 4b and 6b,d). Conversely, the negative influences of anthropogenic water consumption dominated runoff decreases in the agricultural area during 1986–2020 (Figures 4c and 6c,d). The positive influence of climate change on observed runoff changes was evident after the period 2006–2015 in both the pastoral area and the agricultural area (Figure 6d). In the same period, the negative influences of anthropogenic water consumption on observed runoff changes were weakened. The trade-off between these two influences then induced a shift in the dominant driver of observed runoff changes.

4. Discussion

Changes and dominant influences of runoff in the UYRB since the mid-1980s remain poorly constrained yet crucial for ensuring ecological protection and high-quality development in the Yellow River Basin [6,15,18]. In particular, spatiotemporal differences in runoff changes and its drivers between the agricultural area and the pastoral area are of great concern to policymakers when regulating water resources [2,18]. This study calculated runoff changes using hydrological observations over the past 35 years, and then quantified the individual contributions of climate change, land-use and anthropogenic water consumption using scenario simulations with the process-based SWAT model. Differences between the pastoral and agricultural area in terms of runoff changes and its drivers were further analyzed at different temporal scales using hydrological statistical datasets. Compared with the statistical results in previous studies at the entire watershed scale [2,3,19,21], the results reported in our study are reliable and detailed and are expected to provide crucial support for optimizing water resource management in the Yellow River Basin. Additionally, this approach used in our study was well applied to the parts of the Tibetan Plateau and its surroundings that were the source of the Yangtze, Mekong, Indus, Ganges, Amu Darya Rivers, etc. [22,24,40], and provided a potential way to clarify the drivers of runoff changes in these river source regions that have extremely important function of water conservation.

The UYRB, as the most important water source area of the Yellow River Basin and an exoreic basin of the Asia water tower, plays a key role in maintaining water supplies for socioeconomic development locally and downstream [2–4,40]. The observed runoff of the UYRB has reduced since 1986 when compared with that of the period of 1965–1985, mainly due to climate change and anthropogenic water consumption during the same period. This result of our study supports similar findings in previous studies [2,3,15,16]. However, the contribution of land-use change to runoff changes in the UYRB was small, due to the stable land-use pattern. The land-use and land-cover changes, associated with a series of ecological conservation and restoration programs, were mainly observed in the middle and lower reaches the Yellow River, where they markedly reduced the runoff and sediment load in that region [2,4,6,10]. Therefore, sustainable water resource supply remains a challenge in the Yellow River Basin [6,16,40]. The strengthening of water-saving measures provides a feasible solution to mitigate the problem of supply and demand, especially in the agricultural area of the UYRB where runoff changes have been mainly caused by agricultural irrigation and reservoir regulation since 1986 [3,6]. Similarly, the water-saving measures are also workable path to alleviate water resource conflicts in the exoreic basins of the Asia water tower regions, such as the Indus and Amu Darya River basins, where water demands of its downstream regions and countries accelerate in the future [40]. Furthermore, additional feasible policies for sustainable water resource management are urgent to be formulated based on driving mechanisms of runoff changes, which required combinations of improved hydrological modeling and comprehensive observations [14,40,41].

Meltwater runoff from perennial glaciers and frozen soil was not considered in this study and could contribute to the uncertainty in simulated runoff. However, the meltwater would have tended to increase runoff, whereas water loss was also increasing, due to increases in evapotranspiration and reservoir drainage [13,16]. The impacts of meltwater on the changes of total runoff were thus unobvious [3,16]. Moreover, the simulated runoff

series in this study was highly consistent with the observations from hydrological stations in both the calibration and validation periods. Therefore, any uncertainty associated with neglecting the meltwater contribution had little influence on conclusions of this study.

5. Conclusions

The runoff observed at stations in the UYRB appeared to be reduced during 1986–2020 when compared with that in the baseline period of 1965–1985. Similarly, the characteristics of the observed runoff changes were also found in the runoff series for pastoral areas and agricultural areas during the corresponding periods. However, the dominant drivers of the observed runoff changes in these areas showed clear spatiotemporal heterogeneity, identified by comparing contributions from the different influences in scenario simulations with the SWAT model. Climate change had a negative influence and mainly caused the observed runoff reductions in the pastoral area, while anthropogenic water consumption mainly caused the reduced runoff in the agricultural area. The contribution of land-use changes to runoff changes was unobvious due to the stable land-use pattern. Climate change and anthropogenic water consumption were the negative influences that together caused the observed runoff reduction across the entire UYRB over the past 35 years. A shift in the dominant influences occurred in the UYRB after the period of 2006–2015, as the influence of climate change became positive and anthropogenic water consumption was reduced, resulting in the increase in observed runoff since 2016. Improvement of the SWAT model by integrating the processes of meltwater runoff will be performed to accurately predict dynamics in the dominant drivers in such water conservation areas as the UYRB under future development scenarios.

Author Contributions: Conceptualization, F.Z. and B.Z.; methodology, W.Z.; software, K.Y.; validation, F.Z., B.Z. and C.C.; formal analysis, C.C.; investigation, F.Z.; resources, B.Z.; data curation, K.Y.; writing—original draft preparation, F.Z.; writing—review and editing, B.Z.; visualization, W.Z.; supervision, F.Z.; project administration, B.Z.; funding acquisition, B.Z. All authors have read and agreed to the published version of the manuscript.

Funding: This research was funded by the National Natural Science Foundation of China, grant number 42171274.

Data Availability Statement: The data presented in this study are available on request from the corresponding author.

Acknowledgments: The authors thank the editor and three anonymous reviewers for their constructive suggestions to improve the quality of the manuscript and Fang Li for providing materials used for this paper.

Conflicts of Interest: The authors declare no conflict of interest.

References

1. Tang, Q.; Lan, C.; Su, F.; Liu, X.; Sun, H.; Ding, J.; Wang, L.; Leng, G.; Zhang, Y.; Sang, Y.; et al. Streamflow change on the Qinghai-Tibet Plateau and its impacts. *China Sci. Bull.* **2019**, *64*, 807–2821. [[CrossRef](#)]
2. Yang, D.; Yang, Y.; Gao, G.; Huang, J.; Jiang, E. Water Cycle and Soil-water Coupling Processes in the Yellow River Basin. *Bull. Natl. Nat. Sci. Found. China* **2021**, *35*, 544–551. [[CrossRef](#)]
3. Wang, X.; Li, H.; Chen, R.; Liu, J.; Liu, G.; Han, C. Runoff evolution characteristics and driving factors of Yellow River above Lanzhou station from 1956 to under changing environment. *Adv. Earth Sci.* **2022**, *37*, 726–741.
4. Liu, Y.; Song, H.; An, Z.; Sun, C.; Trouet, V.; Cai, Q.; Liu, R.; Leavitt, S.W.; Song, Y.; Li, Q.; et al. Recent anthropogenic curtailing of Yellow River runoff and sediment load is unprecedented over the past 500 y. *Proc. Natl. Acad. Sci. USA* **2020**, *117*, 18251–18257. [[CrossRef](#)] [[PubMed](#)]
5. Grafton, R.; Pittock, J.; Davis, R.; Williams, J.; Fu, G.; Warburton, M.; Udall, B.; McKenzie, R.; Yu, X.; Che, N.; et al. Global insights into water resources, climate change and governance. *Nat. Clim. Change* **2013**, *3*, 315–321. [[CrossRef](#)]
6. Ma, Z.; Fu, C.; Zhou, T.; Yan, Z.; Li, M.; Zheng, Z.; Chen, L.; Lv, M. Status and Ponder of Climate and Hydrology Changes in the Yellow River Basin. *Bull. Chin. Acad. Sci.* **2020**, *35*, 52–60. [[CrossRef](#)]
7. Shi, F.; Liu, S.; Sun, Y.; An, Y.; Zhao, S.; Liu, Y.; Li, M. Ecological network construction of the heterogeneous agro-pastoral areas in the upper Yellow River basin. *Agric. Ecosyst. Environ.* **2020**, *302*, 107069. [[CrossRef](#)]

8. Piao, S.; Ciais, P.; Huang, Y.; Shen, Z.; Peng, S.; Li, J.; Zhou, L.; Liu, H.; Ma, Y.; Ding, Y.; et al. The impacts of climate change on water resources and agriculture in China. *Nature* **2010**, *467*, 43–51. [[CrossRef](#)]
9. Zhao, J.; Mu, X.; Gao, P. Dynamic response of runoff to soil and water conservation measures and precipitation based on VAR model. *Hydrol. Res.* **2019**, *50*, 837–848. [[CrossRef](#)]
10. Li, C.; Zhang, Y.; Shen, Y.; Yu, Q. Decadal water storage decrease driven by vegetation changes in the Yellow River Basin. *Sci. Bull.* **2020**, *65*, 1859–1861. [[CrossRef](#)]
11. Shao, Q.; Fan, J.; Liu, J.; Han, L.; Cao, W.; Liu, L. Target-based Assessment on Effects of First-stage Ecological Conservation and Restoration Project in Three-river Source Region, China and Policy Recommendations. *Bull. Chin. Acad. Sci.* **2017**, *32*, 35–44. [[CrossRef](#)]
12. Wang, Y.; Chen, Y.; Wang, H.; Lv, Y.; Hao, Y.; Cui, X.; Wang, Y.; Hu, R.; Xue, K.; Fu, B. Ecosystem Change and Its Ecohydrological Effect in the Yellow River Basin. *Bull. Natl. Nat. Sci. Found. China* **2021**, *35*, 520–528. [[CrossRef](#)]
13. Wu, P.; Liang, S.; Wang, X.; Feng, Y.; McKenzie, J.M. Climate-induced hydrologic change in the source region of the yellow river: A new assessment including varying permafrost. *Hydrol. Earth Syst. Sci. Discuss.* **2018**, 1–35. [[CrossRef](#)]
14. Yao, T.; Wu, G.; Xu, B.; Wang, W.; Gao, J.; An, B. Asian Water Tower Change and Its Impacts. *Bull. Chin. Acad. Sci.* **2019**, *34*, 1203–1208. [[CrossRef](#)]
15. Liu, C.; Tian, W.; Liu, X.; Liang, K.; Bai, P. Analysis and understanding of runoff variation of the Yellow River in recent 100 years. *Yellow River* **2019**, *41*, 12–16. [[CrossRef](#)]
16. Zheng, Z.; LV, M.; Ma, Z. Climate, Hydrology, and Vegetation Coverage Changes in Source Region of Yellow River and Countermeasures for Challenges. *Bull. Chin. Acad. Sci.* **2020**, *35*, 61–72. [[CrossRef](#)]
17. Zhang, R.; Corte-Real, J.; Moreira, M.; Kilsby, C.; Birkinshaw, S.; Burton, A.; Fowler, H.J.; Forsythe, N.; Nunes, J.P.; Sampaio, E.; et al. Downscaling climate change of water availability, sediment yield and extreme events: Application to a mediterranean climate basin. *Int. J. Climatol.* **2019**, *39*, 2947–2963. [[CrossRef](#)]
18. Fu, B.; Wang, S.; Shen, Y.; Chen, C.; Li, Y.; Feng, X.; Liu, Y. Mechanisms of Human-natural System Coupling and Optimization of the Yellow River Basin. *Bull. Natl. Nat. Sci. Found. China* **2021**, *35*, 504–509. [[CrossRef](#)]
19. Lv, M.; Ma, Z.; Lv, M. Effects of climate/land surface changes on streamflow with consideration of precipitation intensity and catchment characteristics in the Yellow River Basin. *J. Geophys. Res. Atmos.* **2018**, *123*, 1942–1958. [[CrossRef](#)]
20. Schaake, J.C. From climate to flow. In *Climate Change and U.S. Water Resources*; Waggoner, P.E., Ed.; John Wiley: New York, NY, USA, 1990; pp. 177–206.
21. Yang, D.; Zhang, S.; Lu, X. Attribution analysis for runoff decline in Yellow River Basin during past fifty years based on Budyko hypothesis. *Sci. Sin. Technol.* **2015**, *45*, 1024–1034. [[CrossRef](#)]
22. Luo, K. Contribution of ecological conservation programs and climate change to hydrological regime change in the source region of the Yangtze River in China. *Reg. Environ. Change* **2022**, *22*, 1–14. [[CrossRef](#)]
23. Wang, S.; McVicar, T.R.; Zhang, Z.; Brunner, T.; Strauss, P. Globally partitioning the simultaneous impacts of climate-induced and human-induced changes on catchment streamflow: A review and meta-analysis. *J. Hydrol.* **2020**, *590*, 125387. [[CrossRef](#)]
24. Luo, K.; Tao, F.; Moiwu, J.P.; Xiao, D. Attribution of hydrological change in Heihe River Basin to climate and land use change in the past three decades. *Sci. Rep.* **2016**, *6*, 33704. [[CrossRef](#)] [[PubMed](#)]
25. Wang, G.; Xia, J.; Li, X.; Yang, D.; Hu, Z.; Sun, S.; Sun, X. Critical advances in understanding ecohydrological processes of terrestrial vegetation: From leaf to watershed scale. *Chin. Sci. Bull.* **2021**, *66*, 3667–3683. [[CrossRef](#)]
26. Fu, G.; Charles, S.P.; Viney, N.R.; Chen, S.; Wu, J.Q. Impacts of climate variability on stream-flow in the Yellow River. *Hydrol. Processes* **2007**, *21*, 3431–3439. [[CrossRef](#)]
27. Arnold, J.G.; Fohrer, N. SWAT2000: Current capabilities and research opportunities in applied watershed modelling. *Hydrol. Processes* **2005**, *19*, 563–572. [[CrossRef](#)]
28. Lee, S.; Yeo, I.Y.; Lang, M.W.; McCarty, G.W.; Sadeghi, A.M.; Sharifi, A.; Jin, H.; Liu, Y. Improving the catchment scale wetland modeling using remotely sensed data. *Environ. Model. Softw.* **2019**, *122*, 104069. [[CrossRef](#)]
29. Liu, J.; Long, A.; Deng, X.; Yin, Z.; Den, M.; An, Q.; Gu, X.; Li, S.; Liu, G. The Impact of Climate Change on Hydrological Processes of the Glacierized Watershed and Projections. *Remote Sens.* **2022**, *14*, 1314. [[CrossRef](#)]
30. Fu, G.; Chen, S.; Liu, C.; Shepard, D. Hydro-Climatic Trends of the Yellow River Basin for the last 50 years. *Clim. Change* **2004**, *65*, 149–178. [[CrossRef](#)]
31. Gao, S.; Duan, R.; Wang, H.; Li, A.; Shi, Y.; Jing, H.; Fang, J. Farming-Pastoral ecotone of Northern China plays important role in ensuring national food security. *Bull. Chin. Acad. Sci.* **2021**, *36*, 643–650. [[CrossRef](#)]
32. FAO/IIASA/ISRIC/ISSCAS/JRC. *Harmonized World Soil Database Version 1.2*; FAO: Rome, Italy; IIASA: Laxenburg, Austria, 2012.
33. Winchell, M.; Srinivasan, R.; Di Luzio, M.; Arnold, J. *ArcSWAT Interface for SWAT2009 User's Guide*; Texas Agricultural Experiment Station and U.S. Department of Agriculture: Temple, TX, USA, 2010.
34. Tachikawa, T.; Hato, M.; Kaku, M.; Iwasaki, A. The Characteristics of ASTER GDEM Version 2. In Proceedings of the 2011 IEEE International Geoscience and Remote Sensing Symposium, IGARSS, Vancouver, BC, Canada, 24–29 July 2011.
35. Arnold, J.G.; Srinivasan, R.; Muttiah, R.S.; Williams, J.R. Large area hydrologic modeling and assessment part I: Model development. *J. Am. Water Resour. Assoc.* **1998**, *34*, 73–89. [[CrossRef](#)]
36. Neitsch, S.L.; Arnold, J.G.; Kiniry, J.R.; Williams, J.R. *Soil and Water Assessment Tool Theoretical Documentation Version 2009*; Texas Water Resources Institute Technical Report; Texas A&M University System: College Station, TX, USA, 2011.

37. Abbaspour, K.; Vaghefi, S.; Srinivasan, R. A Guideline for Successful Calibration and Uncertainty Analysis for Soil and Water Assessment: A Review of Papers from the 2016 International SWAT Conference. *Water* **2017**, *10*, 6. [[CrossRef](#)]
38. Guzman, J.A.; Shirmohammadi, A.; Sadeghi, A.M.; Wang, X.; Chu, M.L.; Jha, M.; Parajuli, P.B.; Harmel, R.D.; Khare, Y.; Hernandez, J.E. Uncertainty Considerations in Calibration and Validation of Hydrologic and Water Quality Models. *Trans. ASABE* **2015**, *58*, 1745–1762. [[CrossRef](#)]
39. Moriasi, D.N.; Arnold, J.G.; Van Liew, M.W.; Bingner, R.L.; Harmel, R.D.; Veith, T.L. Model evaluation guidelines for systematic quantification of accuracy in watershed simulations. *Trans. ASABE* **2007**, *50*, 885–900. [[CrossRef](#)]
40. Yao, T.; Bolch, T.; Chen, D.; Gao, J.; Immerzeel, W.; Piao, S.; Su, F.; Thompson, L.; Wada, Y.; Wang, L.; et al. The imbalance of the Asian water tower. *Nat. Rev. Earth Environ.* **2022**. [[CrossRef](#)]
41. Yu, G.; Zhang, L.; Zhang, Y.; Yang, M. A coordinated three-dimensional network for observing large-scale terrestrial ecosystem status changes and the consequences on resources and environment. *Chin. J. Appl. Ecol.* **2021**, *32*, 6. [[CrossRef](#)]